Quasiparticle bandstructure of antiferromagnetic EuTe

1997 J. Phys.: Condens. Matter 9 10439

(http://iopscience.iop.org/0953-8984/9/47/012)

J. Phys.: Condens. Matter **9** (1997) 10439–10456. Printed in the UK PII: S0953-8984(97)85685-8

Quasiparticle bandstructure of antiferromagnetic EuTe

S Mathi Jaya and W Nolting

Humboldt-Universität zu Berlin, Institut für Physik, Lehrstuhl Festkörpertheorie, Invalidenstrasse 110, D-10115 Berlin, Germany

Received 30 June 1997, in final form 9 September 1997

Abstract. The temperature-dependent electronic quasiparticle spectrum of the antiferromagnetic semiconductor EuTe is derived by use of a combination of a many-body model procedure with a tight-binding–'linear muffin tin orbital' (TB–LMTO) band structure calculation. The central part is the d–f model for a single band electron ('test electron') being exchange coupled to the antiferromagnetically ordered localized moments of the Eu ions. The single-electron Bloch energies of the d–f model are taken from a TB–LMTO calculation for paramagnetic EuTe. The d–f model is evaluated by a recently proposed moment conserving Green function technique to get the temperature-dependent sublattice–quasiparticle bandstructure (S–QBS) and sublattice–quasiparticle density of states (S–QDOS) of the unoccupied 5d–6s energy bands. Unconventional correlation effects and the appearance of characteristic quasiparticles ('magnetic polarons') are worked out in detail. The temperature dependence of the S–QDOS and S–QBS is mainly provoked by the spectral weights of the energy dispersions. Minority- and majority-spin spectra coincide for all temperatures but with different densities of states. Upon cooling from T_N to $T = 0$ K the lower conduction band edge exhibits a small blue shift of -0.025 eV in accordance with the experiment. Quasiparticle damping manifesting itself in a temperature-dependent broadening of the spectral density peaks arises from spin exchange processes between (5d–6s) conduction band electrons and localized 4f moments.

1. Introduction

The europium monochalcogenides EuX (X = O, S, Se, Te) have attracted scientific interest as have very few other groups of solid compounds. All the EuX compounds [1, 2] crystallize in the rocksalt structure where the Eu^{2+} ions occupy the sites of an fcc structure. As to their purely magnetic properties they may be considered as sufficiently well understood. They are almost ideal realizations of the isotropic Heisenberg exchange model. The oxide and sulphide are ferromagnets, the selenide is a metamagnet and the telluride is a prototypical antiferromagnet [1, 3–5]. The magnetic moment of 7 μ_B stems from the exactly half-filled and strictly localized 4f shell of the Eu^{2+} ion ($L = 0$, $J = S = 7/2$). The magnetic structure of antiferromagnetic EuTe is that of MnO, i.e., the (111) planes order ferromagnetically with alternating magnetization directions between adjacent planes. EuTe has a Néel temperature of 9.6 K and a negative paramagnetic Curie temperature of -4 K.

Many striking properties of magnetic semiconductors like the EuX are provoked by an interband exchange interaction between the localized 4f electrons and itinerant (5d, 6s) charge carriers. At low temperatures, it is sufficient to assume a single electron ('test electron') in an otherwise empty conduction band. The first experimentally observed exchange effect is the 'red shift' of the optical absorption edge upon cooling a ferromagnetic semiconductor below the Curie temperature [6]. For antiferromagnetic semiconductors the situation is not so clear: some exhibit a red shift (EuSe, $ZrCr_2Se_4$), others a blue shift

0953-8984/97/4710439+18$19.50

(EuTe, $NaCr_2Se_4$) [6, 7]. In any case the effect documents a striking temperature-dependent electronic structure which has to be traced back to the already mentioned 4f–(5d, 6s) exchange coupling. Other experiments of which the results are determined by this interaction concern the spin-filter properties of EuS–W junctions [8, 9], the insulator–metal transition in Eu-rich EuO [10], the band filling dependence of the EuO Curie temperature [11] and the pressure induced intermediate valence state of the Eu^{2+} ion in EuO, EuS [12, 13]. A proper theoretical model for an at least qualitative description of these experimental findings is the s–f (s–d) model [14, 15]. The model Hamiltonian

$$H = H_s + H_f + H_{sf} \tag{1}$$

describes the mutual influence of localized (H_f) and itinerant (H_s) electrons via an interband exchange interaction H_{sf}. The model is able to demonstrate how the magnetic state of the localized f system may lead to drastic temperature dependences of the conduction band states, to shifts, deformations and splittings of the empty band [14–16]. On the other hand, a finite band filling drastically affects the magnetic behaviour of the moment system [17], in particular the type of the magnetic order, the magnetization and the critical temperatures.

In this paper, we restrict our considerations to the conduction band structure of the antiferromagnet EuTe. This empty band is built up by (5d–6s) states of the Eu^{2+} ion. The seven 4f electrons of the Eu^{2+} ion enter our model description only as permanent magnetic moments of 7 μ_B. We investigate how the temperature-dependent sublattice magnetization manifests itself in the electronic quasiparticle spectrum. For a quantitative comparison with the experimental data, however, the bare s–f model is of course overtaxed since all interactions, except for the mentioned 4f–(5d–6s) exchange, are suppressed. To incorporate the consequences of the neglected interactions in an averaged, but rather realistic manner, we have proposed in a series of preceding papers [18–22] a method which combines the results of a self-consistent band structure calculation based on the density-functional theory with a reliable many-body treatment of the s–f model to get realistic predictions for the temperature-dependent quasiparticle band structure of local-moment ferromagnets such as EuO, EuS and Gd. We extend in this paper the mentioned method to the prototypical Heisenberg antiferromagnet EuTe. After defining in a proper way the sublattice structure of EuTe and the magnetic unit cell we perform a 'tight-binding–linear muffin tin orbital' (TB–LMTO) calculation for paramagnetic EuTe. The results are taken as the effective single-particle input for the subsequent many-body evaluation of the s–f model. Therewith we guarantee that all the other interactions, which are not directly covered by the theoretical model (1), are taken into account in a sufficiently realistic way. The main problem of this method lies in a possible double-counting of just the decisive interaction, namely the s–f exchange interaction, once explicitly via the model evaluation and then once more implicitly by the renormalized single-particle energies. It is explained later in the text how we circumvent this problem. For the mentioned many-body evaluation of the underlying theoretical model, we apply a moment conserving Green function decoupling technique that has been introduced in a preceding paper [16]. The approach exactly fulfils all relevant limiting cases.

The paper is organized as follows. In the next section, we formulate explicitly the s–f model for an antiferromagnetic semiconductor such as EuTe. In section 3 the Bloch energy matrix is determined by a TB–LMTO calculation for getting the effective single-particle input for the subsequent derivation of the self-energy matrix. The results are presented in section 5 in terms of the temperature-dependent quasiparticle band structures and densities of states. Special attention is devoted to unconventional correlation effects ('magnetic polaron') which manifest themselves in the electronic structure of EuTe.

2. Model description of antiferromagnetic semiconductors

We presume a solid that is composed of m penetrating sublattices α ($\alpha = 1, 2, \ldots, m$). The local moments on each of the chemically equivalent sublattices order ferromagnetically, but with different orientations of the spontaneous magnetization for different α. We consider the total (chemical) lattice as a magnetic Bravais lattice ($\boldsymbol{R}_i$) with an m-atom basis ($\boldsymbol{r}_\alpha$)

$$\boldsymbol{R}_{i\alpha} = \boldsymbol{R}_i + \boldsymbol{r}_a. \tag{2}$$

i numbers the N sites of the Bravais lattice. Translational symmetry holds for each sublattice so that the thermodynamic average of a site-dependent operator $O_{i\alpha}$ only depends on the sublattice index α:

$$\langle O_{i\alpha}\rangle \equiv \langle O_\alpha\rangle. \tag{3}$$

Fourier transformations therefore refer to the magnetic Bravais lattice and the respective Brillouin zone:

$$O_{i\alpha} = \frac{1}{\sqrt{N}} \sum_{\boldsymbol{k}} \mathrm{e}^{\mathrm{i}\boldsymbol{k}\cdot\boldsymbol{R}_i} O_{\boldsymbol{k}\alpha}. \tag{4}$$

For the investigation of an antiferromagnetic semiconductor we apply the s–f model Hamiltonian (1). At each lattice site $\boldsymbol{R}_{i\alpha}$ a permanent magnetic moment is localized, represented by a spin operator $S_{i\alpha}$. The exchange-coupled spins are described by the Heisenberg model:

$$H_f = -\sum_{\substack{ij\\ \alpha\beta}} J_{ij}^{\alpha\beta} \boldsymbol{S}_{ij} \cdot \boldsymbol{S}_{j\beta}. \tag{5}$$

The exchange integrals $J_{ij}^{\alpha\beta}$ determine the magnetic structure. The partial operator H_s refers to the band electrons, in the s–f model being treated as s electrons without Coulomb interaction:

$$H_s = \sum_{\substack{ij\sigma\\ \alpha\beta}} T_{ij}^{\alpha\beta} c_{i\alpha\sigma}^{+} c_{j\beta\sigma} = \sum_{\substack{\boldsymbol{k}\sigma\\ \alpha\beta}} \varepsilon_{\alpha\beta}(\boldsymbol{k}) c_{\boldsymbol{k}\alpha\sigma}^{+} c_{\boldsymbol{k}\beta\sigma}. \tag{6}$$

$c_{i\alpha\sigma}^{+}$ ($c_{\boldsymbol{k}\alpha\sigma}^{+}$) and $c_{i\alpha\sigma}$ ($c_{\boldsymbol{k}\alpha\sigma}$) are, respectively, the creation and the annihilation operator of an electron with spin σ ($\sigma = \uparrow, \downarrow$) at site $\boldsymbol{R}_{i\alpha}$ (with wave-vector $\boldsymbol{k}$ in sublattice α). $T_{ij}^{\alpha\beta}$ is the hopping matrix and $\varepsilon_{\alpha\beta}(\boldsymbol{k})$ the corresponding Bloch energy matrix:

$$T_{ij}^{\alpha\beta} = \frac{1}{N} \sum_{\boldsymbol{k}} \varepsilon_{\alpha\beta}(\boldsymbol{k})\, \mathrm{e}^{\mathrm{i}\boldsymbol{k}\cdot(\boldsymbol{R}_i - \boldsymbol{R}_j)}. \tag{7}$$

Our study aims at the electronic quasiparticle spectrum of the semiconductor EuTe. We therefore assume a single electron ('test electron') in an otherwise empty conduction band so that the neglect of the Coulomb interaction in (6) is trivially justified. The itinerant electron interacts with the localized spin system via an intra-atomic exchange H_{sf}:

$$H_{sf} = -J \sum_{j\alpha} \boldsymbol{\sigma}_{j\alpha} \cdot \boldsymbol{S}_{j\alpha} = -\frac{1}{2} J \sum_{j\alpha\sigma} (z_\sigma S_{j\alpha}^{z} n_{j\alpha\sigma} + S_{j\alpha}^{\sigma} c_{j\alpha-\sigma}^{+} c_{j\alpha\sigma}). \tag{8}$$

$\boldsymbol{\sigma}_{j\alpha}$ is the electron spin operator and $n_{j\alpha\sigma} = c_{j\alpha\sigma}^{+} c_{j\alpha\sigma}$ the occupation number operator. J is the s–f coupling constant. For abbreviation we use

$$S_{j\alpha}^{\sigma} = S_{j\alpha}^{x} + \mathrm{i} z_\sigma S_{j\alpha}^{y} \qquad z_\uparrow = +1, z_\downarrow = -1. \tag{9}$$

The relevant information with respect to the electronic quasiparticle spectrum can be drawn from the retarded single-electron Green function:

$$G_{ij\sigma}^{\alpha\beta}(E) = \langle\langle c_{i\alpha\sigma}; c_{j\beta\sigma}^{+}\rangle\rangle_E = -\mathrm{i}\int_0^\infty \mathrm{d}t\, \mathrm{e}^{-\mathrm{i}/\hbar Et}\langle[c_{i\alpha\sigma}(t), c_{j\beta\sigma}^{+}(0)]_+\rangle. \tag{10}$$

$[\ldots,\ldots]_+$ ($[\ldots,\ldots]_-$) means the anticommutator (commutator) and $\langle\ldots\rangle$ the thermodynamic average. The equation of motion of the Green function,

$$\sum_{r,\gamma}(E\delta_{ir}\delta_{\alpha\gamma} - T_{ir}^{\alpha\gamma})G_{rj\sigma}^{\gamma\beta}(E) = \hbar\delta_{ij}\delta_{\alpha\beta} + \langle\langle[c_{i\alpha\sigma}, H_{sf}]_-; c_{j\beta\sigma}^{+}\rangle\rangle_E \tag{11}$$

can be used to define the self-energy matrix $M_{ij\sigma}^{\alpha\beta}(E)$ by

$$\langle\langle[c_{i\alpha\sigma}, H_{sf}]_-; c_{j\beta\sigma}^{+}\rangle\rangle = \sum_{r,\gamma} M_{ir\sigma}^{\alpha\gamma}(E)G_{rj\sigma}^{\gamma\beta}(E). \tag{12}$$

Fourier transformation formally solves the problem. In matrix representation the Green function reads

$$\mathbf{G}_{k\sigma}(E) = \hbar(E - \varepsilon(\boldsymbol{k}) - \mathbf{M}_{k}\sigma(E))^{-1}. \tag{13}$$

The full influence of the exchange interaction is gathered in the self-energy matrix $\mathbf{M}_{k\sigma}(E)$, the determination of which therefore is the central task of our study.

3. Bloch energy matrix

The Eu moments of EuTe build an fcc structure where the moments in the (111) planes are ferromagnetically arranged with alternating directions of the magnetization in adjacent layers. The magnetic unit cell of EuTe may be constructed in different ways. It is clear that for computational convenience the number of atoms per cell should be a minimum. On the other hand, the unavoidable $\boldsymbol{k}$-summations need a magnetic Brillouin zone as simple as possible. Taking these two aspects into consideration we have chosen a base centred orthorhombic magnetic unit cell with the lattice parameters $a = 2a_0$, $b = \sqrt{2a_0}$ and $c = a_0/\sqrt{2}$ (figure 1). a_0 is the lattice constant of the chemical lattice. The magnetic primitive cell accommodates two up-spin and two down-spin Eu atoms. Treating each Eu atom as belonging to a sublattice, we thus get a four-sublattice antiferromagnet. The Bloch energy matrix in (13) and (6), respectively, therefore is a 4×4 matrix. We shall denote the intrasublattice Bloch energy as $\varepsilon(\boldsymbol{k})$ and the intersublattice energies as $t(\boldsymbol{k})$, $u(\boldsymbol{k})$ and $v(\boldsymbol{k})$. Obeying obvious symmetries (figure 1) one gets the following matrix $\varepsilon(\boldsymbol{k})$:

$$\varepsilon(\boldsymbol{k}) \equiv \begin{pmatrix} \varepsilon(\boldsymbol{k}) & t(\boldsymbol{k}) & u(\boldsymbol{k}) & v(\boldsymbol{k}) \\ t(\boldsymbol{k}) & \varepsilon(\boldsymbol{k}) & v(\boldsymbol{k}) & u(\boldsymbol{k}) \\ u(\boldsymbol{k}) & v(\boldsymbol{k}) & \varepsilon(\boldsymbol{k}) & t(\boldsymbol{k}) \\ v(\boldsymbol{k}) & u(\boldsymbol{k}) & t(\boldsymbol{k}) & \varepsilon(\boldsymbol{k}) \end{pmatrix}. \tag{14}$$

The goal is now to evaluate ε, t, u and v. If the crystal has only one s band in the chemical lattice and if the latter is composed of four sublattices than there will be four branches in the band structure of the magnetic lattice. The eigenvalues of the Bloch matrix are nothing else than the four values of the band dispersions at each $\boldsymbol{k}$-point in the first Brillouin zone of the magnetic Bravais lattice. If we perform separately a band-structure calculation, so that we know at each $\boldsymbol{k}$-point the values of the four dispersion curves, and therewith the eigenvalues of the Bloch matrix, then it is possible to determine the above said $\varepsilon(\boldsymbol{k})$, $t(\boldsymbol{k})$, $u(\boldsymbol{k})$, $v(\boldsymbol{k})$ by numerical techniques.

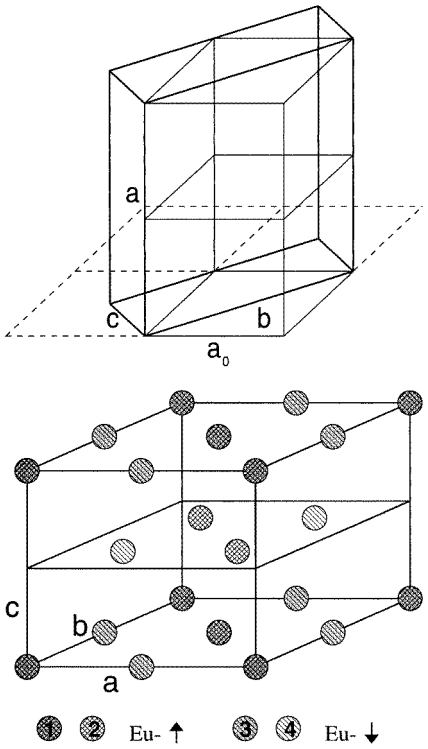

Figure 1. Magnetic unit cell of EuTe. It is a base centred orthorhombic lattice with eight Eu atoms. The four sublattices contained in this structure are shown with four different patterns.

Our study aims at the conduction band of EuTe which consists of five Eu 5d bands and one Eu 6s band. The terms in the preceding formulae thus require an additional band index m that has been left up to now for clarity. We followed the above-described procedure to determine $\varepsilon_m(\boldsymbol{k})$, $t_m(\boldsymbol{k})$, $u_m(\boldsymbol{k})$ and $v_m(\boldsymbol{k})$ from a TB–LMTO bandstructure calculation [23, 24]. The main problem, when using such results as single-particle input for our EuTe theory, arises by a possible double-counting of the s–f exchange interactions, namely once in the single-electron band calculation and then once more explicitly in the following many-body procedure. We circumvent this problem by exploiting the fact which has been worked out by several authors [25, 26] that standard spin-polarized band calculations for magnetic materials are practically consistent with the Stoner model. In the paramagnetic phase, however, the Stoner quasiparticle energies are identical to the 'free' Bloch energies. We have therefore performed the above-mentioned $T = 0$-band calculation for *paramagnetic* EuTe. We believe that all interactions responsible for the 4f induced magnetic behaviour of the conduction bands are then more or less switched off while all the other 'non-magnetic' interactions contribute to a renormalization of the single-particle energies. The result for the *chemical* lattice is plotted in figure 2 where we have chosen the lattice constant to be $a_0 = 4.367$ Å. One recognizes that the flat Eu 4f bands lie between the occupied Te 5p bands and the empty Eu (5d, 6s) conduction bands.

As explained above the evaluation of the Bloch energy matrix needs the calculation of the band structure in the magnetic lattice, which takes care of an additional fourfold splitting.

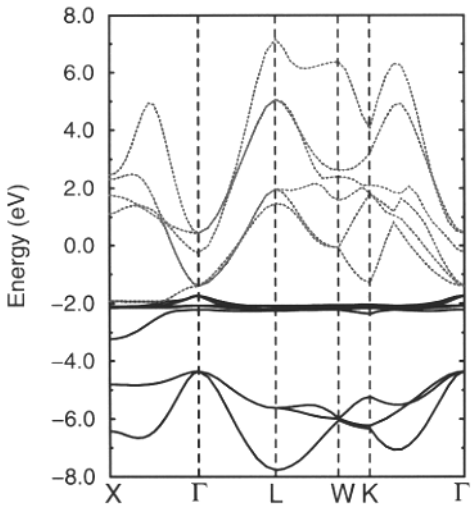

Figure 2. Band structure of EuTe in the *chemical* lattice. The six conduction bands ($m = 1$–6) are shown as dotted lines.

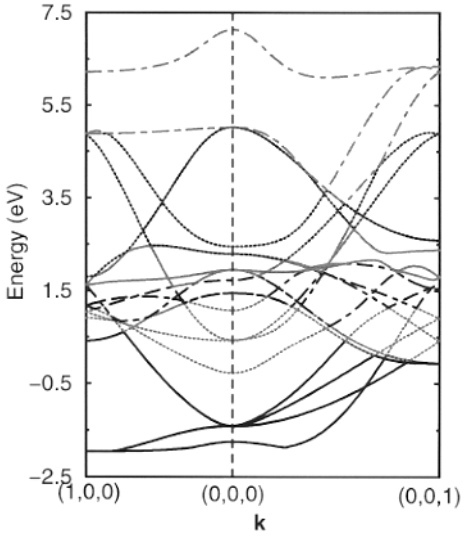

Figure 3. The six conduction bands of the chemical lattice of EuTe which become 24 branches in the magnetic lattice. They are grouped into six sections (shown with different intensity and different line styles). The first section is assumed to constitute the $m = 1$ subband and it is called band 1, the second section is assumed to constitute the $m = 2$ subband and it is called band 2 and so on.

Thus there are altogether 24 branches as can be seen in figure 3. They are grouped into six non-degenerate subbands ($m = 1, 2, \ldots, 6$) according to the following procedure. At each $\boldsymbol{k}$-point of the Brillouin-zone we sort out the 24 energetically lowest conduction band states and number them with respect to increasing single-electron energy. The first four states belong to subband $m = 1$, the next four to subband $m = 2$, and so on. Now we consider the four branches of a given m as the eigenvalues of the Bloch matrix (14) and determine

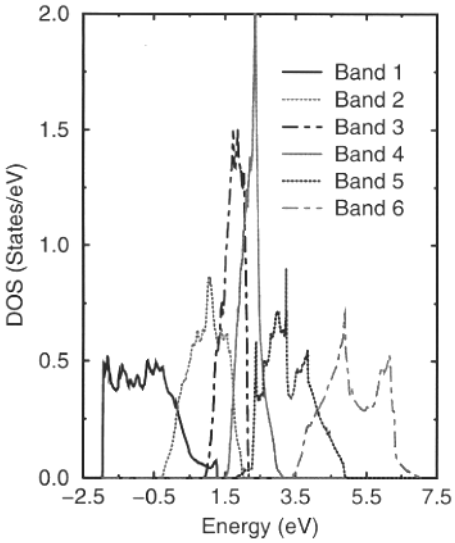

Figure 4. The density of states of EuTe corresponding to all the six sections of the conduction band structure shown in figure 3.

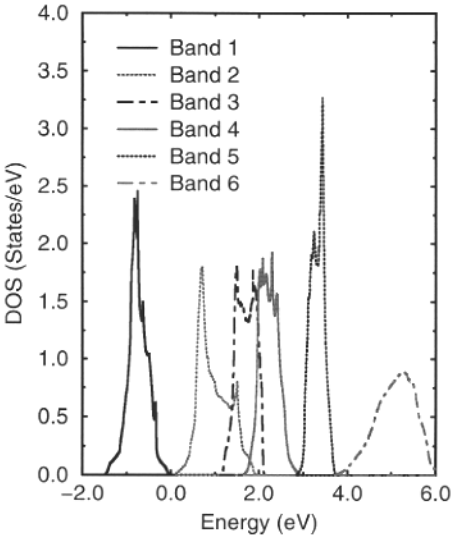

Figure 5. The density of states of the sublattice corresponding to intrasublattice hopping $\varepsilon_m(\boldsymbol{k})$, only; needed for the calculation of the sublattice self-energy (17) and (18), respectively.

the $\varepsilon_m(\boldsymbol{k})$, $t_m(\boldsymbol{k})$, $u_m(\boldsymbol{k})$ and $v_m(\boldsymbol{k})$ at each $\boldsymbol{k}$-point by solving the problem numerically. The procedure is repeated for all the six sections. The Bloch density of states (BDOS) of sublattice α is then calculated according to a matrix inversion of the 'free' Green function

$$\rho^{(0)}_{m\alpha\sigma}(E) = \rho^{(0)}_{m\alpha-\sigma}(E) = -\frac{1}{N\pi}\sum_{\boldsymbol{k}} \mathrm{Im}(E + \mathrm{i}0^+ - \varepsilon_m(\boldsymbol{k}))^{-1}_{\alpha\alpha}. \tag{15}$$

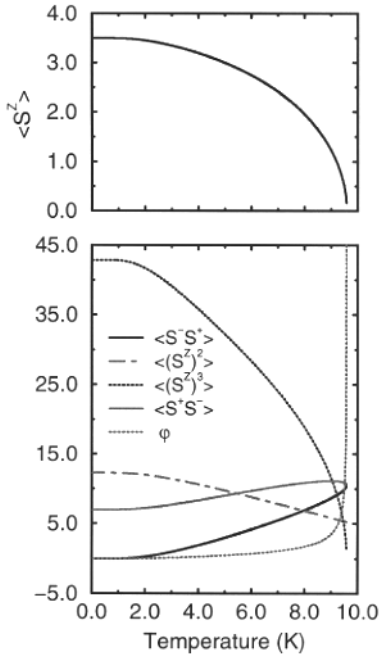

Figure 6. Several spin correlation functions in dependence on temperature for EuTe. The upper part shows the sublattice magnetization.

From symmetry the BDOS is of course the same for all the four sublattices. The sublattice Bloch density of states is plotted in figure 4. For the calculation of the self-energy in the next section, however, we need the BDOS for the special case of intrasublattice hopping, only. In (15) the matrix $\varepsilon_m(\boldsymbol{k})$ has simply to be replaced by the diagonal Bloch energy $\varepsilon_m(\boldsymbol{k})$. This DOS, which is represented in figure 5, has no direct physical meaning, being only an auxiliary quantity for the following treatment. Therewith the single-particle input for the Hamiltonian (1) of the four-sublattice antiferromagnet EuTe is completely defined. In the next step we describe the many-body treatment of the 4f–(5d, 6s) interband exchange interaction.

4. Self-energy matrix

According to the chosen four-sublattice structure the resulting Green function (13) of the interacting particle system will represent a 4×4 matrix and the same is true for the self-energy matrix:

$$\mathbf{M}_{\boldsymbol{k}m\sigma}(E) \equiv (M^{(\alpha\beta)}_{\boldsymbol{k}m\sigma})(E))_{\alpha,\beta=1,\ldots,4}. \tag{16}$$

After having diagonalized the one-particle matrix $\varepsilon_m(\boldsymbol{k})$ (14, 15) with respect to the band index m the self-energy $\mathbf{M}$ will, strictly speaking, be a matrix not only in the sublattice index α, but also in the band index m. For simplicity this fact is disregarded here. Intersubband contributions are assumed to be sufficiently well accounted for by the LMTO input. Because of the special magnetic order (figure 1) and the chemically equivalent sublattices it must hold for the diagonal elements:

$$M^{(11)}_{\boldsymbol{k}m\sigma}(E) = M^{(22)}_{\boldsymbol{k}m\sigma}(E) \equiv M_{m\sigma}(E) \tag{17}$$

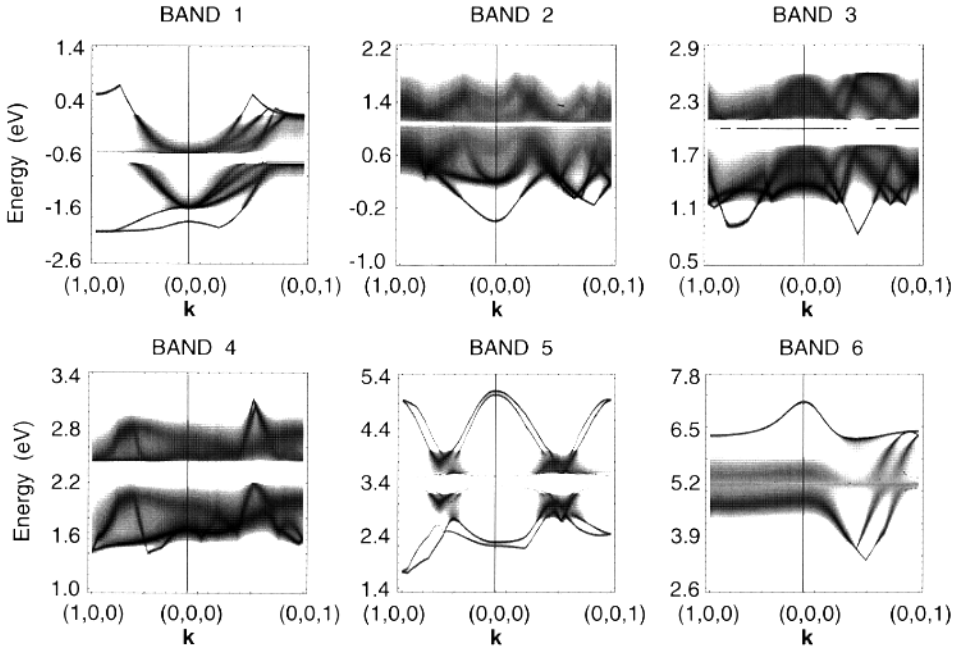

Figure 7. Density plot of the sublattice spectral density (sublattice quasiparticle band structure) of EuTe at $\langle S^z \rangle = 0.0$. The degree of blackening measures the magnitude of the spectral density.

$$M^{(33)}_{\boldsymbol{k}m\sigma}(E) = M^{(44)}_{\boldsymbol{k}m\sigma}(E) \equiv M_{m-\sigma}(E). \tag{18}$$

As explained after (22) our many-body evaluation leads to a $\boldsymbol{k}$-independent (local) self-energy. From this reason the off-diagonal elements of $\mathbf{M}_{m\sigma}$ vanish identically in the paramagnetic phase (translational symmetry in full chemical lattice!). Since the self-energy is provoked by the local exchange interaction (8) acting in the paramagnetic as well as in the antiferromagnetic phase it is plausible to assume that the off-diagonal elements play only a minor role in the ordered phase, too:

$$M^{(\alpha\beta)}_{m\sigma}(E) \approx 0 \qquad \text{for } \alpha \neq \beta. \tag{19}$$

Using the short-hand notation

$$A_{\boldsymbol{k}m\sigma}(E) \equiv E - \varepsilon_m(\boldsymbol{k}) - M_{m\sigma}(E) \tag{20}$$

the approximate Green function matrix in the four-sublattice structure reads:

$$\overline{h}\mathbf{G}^{-1}_{\boldsymbol{k}m\sigma}(E) \equiv \begin{pmatrix} A_{\boldsymbol{k}m\sigma}(E) & -t_m(\boldsymbol{k}) & -u_m(\boldsymbol{k}) & -v_m(\boldsymbol{k}) \\ -t_m(\boldsymbol{k}) & A_{\boldsymbol{k}m\sigma}(E) & -v_m(\boldsymbol{k}) & -u_m(\boldsymbol{k}) \\ -u_m(\boldsymbol{k}) & -v_m(\boldsymbol{k}) & A_{\boldsymbol{k}m-\sigma}(E) & -t_m(\boldsymbol{k}) \\ -v_m(\boldsymbol{k}) & -u_m(\boldsymbol{k}) & -t_m(\boldsymbol{k}) & A_{\boldsymbol{k}m-\sigma}(E) \end{pmatrix}. \tag{21}$$

The only quantity to be determined is the self-energy $M_{\boldsymbol{k}m\sigma}(E)$ of the ferromagnetic sublattice. We derive it from a respective treatment of a ferromagnetic semiconductor [10] neglecting therewith the influence of intersublattice hopping on the sublattice self-energy. The intersublattice hopping appears explicitly in the Green function matrix (21) via u_m, v_m, t_m. So our *ansatz* is correct in first order of the intersublattice hopping. That this is indeed an acceptable assumption has been demonstrated in [27] for the antiferromagnetic

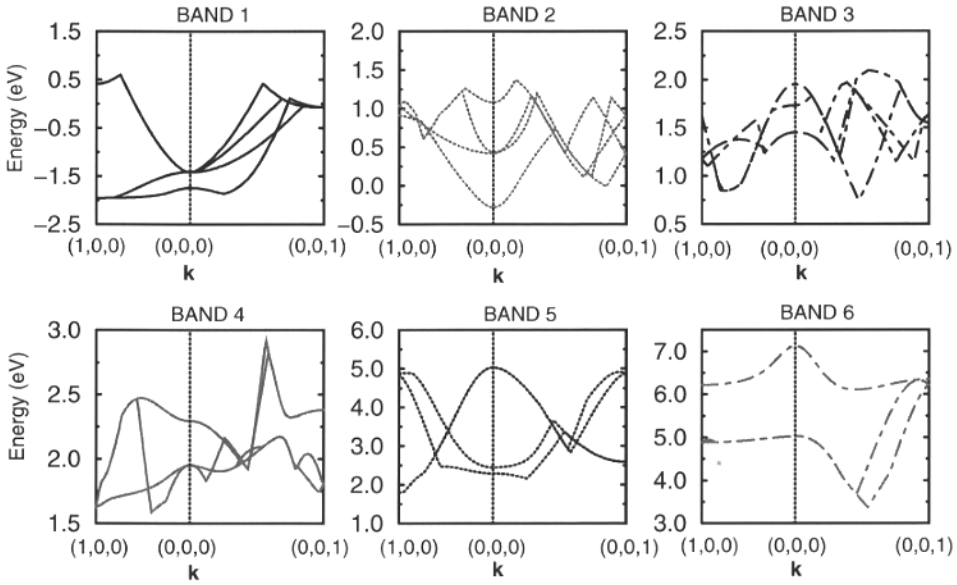

Figure 8. Separate plotting of the six sections of the conduction band structure of EuTe shown in figure 3.

single-band Hubbard model. It has also been applied in our previous paper [16] to a model antiferromagnetic semiconductor with a two-sublattice structure. From that treatment we exploit furthermore the moment conserving decoupling procedure to perform the explicit derivation of the ferromagnetic self-energy $M_{\boldsymbol{k}m\sigma}(E)$. Thus we can restrict ourselves here to comment only on the resulting expression that enters the Green function matrix (20). For the details of the mathematical evaluation the reader is referred to [16]. The rough structure of the self-energy can be formulated as follows:

$$M_{m\sigma}(E) = -\tfrac{1}{2}J_m z_\sigma \langle S^z\rangle + \tfrac{1}{4}J_m^2 Q_{m\sigma}(E). \tag{22}$$

$\langle S^z\rangle$ is the 4f-sublattice magnetization. A possible $\boldsymbol{k}$-dependence of the self-energy comes into play exclusively by the magnon dispersion of the local magnetic moment system. Magnon energies are smaller by several orders of magnitude than other typical energies of the system, e.g., the bandwidth or the s–f coupling constant J, although, being not necessary for solving the equations [17], we neglected the magnon energies, getting therewith a wave-vector-independent electronic self-energy.

The first term in (22) describes a Stoner-like induced exchange splitting of the conduction band states which disappears in the paramagnetic phase. In weakly coupled systems it dominates the temperature dependence of the states in a ferromagnetic semiconductor. It turns out to be the correct leading term even in the case of finite band occupations (metals!) [17]. A Stoner-like exchange splitting has been observed for certain positions in the Brillouin zone of Gd by use of spin-polarized photoemission [28]. It is an open and controversially discussed question whether or not the linear term in (22) is dominant for all interesting magnetic semiconductors and local-moment metals.

The second part of the self-energy (22) is a very complicated functional of the self-energy itself for both spin directions and of local spin correlation functions of the localized 4f-moment system ($\langle S_\alpha^z\rangle$, $\langle S_\alpha^\pm S_\alpha^\mp\rangle$, ...). The equations (44) to (47) together with the equations (37) to (39) in [16] represent the full expression of the self-energy. A detailed inspection of

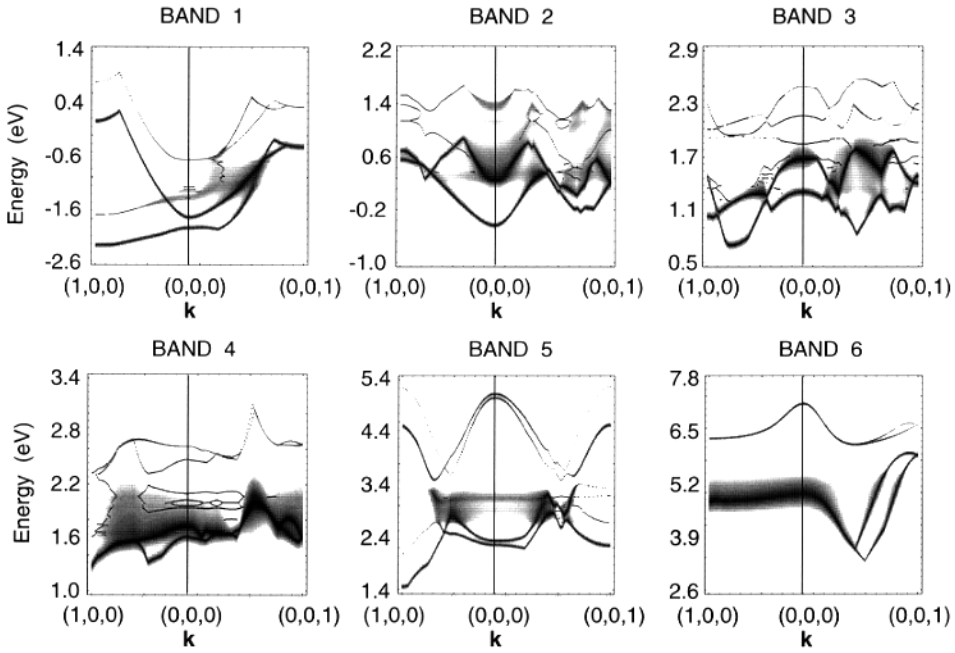

Figure 9. Density plot of the sublattice spectral density (sublattice quasiparticle band structure) of EuTe corresponding to up spin at $\langle S^z \rangle = S$. The degree of blackening measures the magnitude of the spectral density.

the second term in the self-energy result (22) reveals that it is mainly caused by spin exchange processes between the conduction electron and the localized moment system mediated by the corresponding spinflip operator in the s–f exchange interaction (8). For low temperatures it tends to reduce the induced first-order exchange splitting. For higher temperatures, slightly below or above the transition point, it can cause a persistent splitting of the band states even in the paramagnetic phase. In the next section we will find some indications that this is indeed the case in certain parts of the EuTe Brillouin zone. The local spin correlation functions can all be expressed by the sublattice magnetization $\langle S_\alpha^z \rangle$ applying a method described in [16].

For a given temperature we iterate the sublattice self-energy via (22) up to the desired accuracy. The result is inserted into the Green-function matrix (21). Its diagonal elements are determined according to

$$(S_{km\sigma}(E))_{\alpha\alpha} = -\frac{1}{\pi}\,\mathrm{Im}((E - \varepsilon_m(\boldsymbol{k}) - \mathbf{M}_{km\sigma}(E))^{-1})_{\alpha\alpha} \tag{23}$$

the sublattice spectral density, the prominent peaks of which help to define the temperature-dependent sublattice quasiparticle bandstructure. The quasiparticle density of states of the four sublattices results from an additional wave-vector summation over the first Brillouin zone of the magnetic Bravais lattice:

$$\rho_{m\alpha\sigma}(E) = \frac{1}{N}\sum_{\boldsymbol{k}}(S_{km\sigma}(E))_{\alpha\alpha}. \tag{24}$$

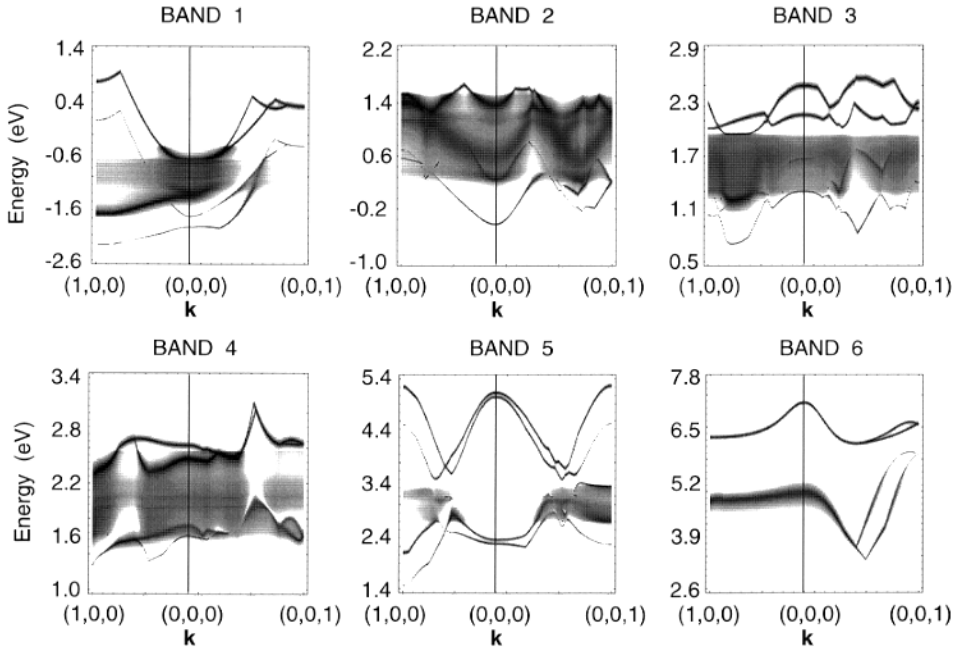

Figure 10. Same as in figure 9 but for the down spin.

It is clear that the functions for $\alpha = 1$ and $\alpha = 2$ are identical while for the two others the symmetry

$$(\alpha = 1,\ 2;\ \sigma) \leftrightarrow (\alpha = 3,\ 4;\ -\sigma) \tag{25}$$

holds. The representation can therefore be restricted to the $\alpha = 1$ functions.

5. Discussion of the results

EuTe can be considered as a prototype of a Heisenberg antiferromagnet. The empty conduction band of the insulator (semiconductor) has no influence on the magnetic properties of the localized 4f spin system, so that the sublattice-magnetization curve turns out to be very similar to a simple Brillouin function. We therefore treat the sublattice magnetization $\langle S_\alpha^z \rangle$ as a given temperature-dependent parameter, realized by an $S = 7/2$ Brillouin function according to the EuTe transition temperature $T_N = 9.6$ K. As explained in [16] we can use $\langle S_\alpha^z \rangle$ to derive from the following formula [29]

$$\langle S_\alpha^z \rangle = \frac{(1 + S + \varphi)\varphi^{2S+1} + (S - \varphi)(1 + \varphi)^{2S+1}}{(1 + \varphi)^{2S+1} - \varphi^{2S+1}} \tag{26}$$

the quantity $\varphi = \varphi(S)$ which has the meaning of an average magnon number per site. This term helps to express the other local spin correlations needed for the evaluation of the sublattice self-energy (22):

$$\langle S_\alpha^- S_\alpha^+ \rangle = 2\overline{h}\langle S_\alpha^z \rangle \varphi \tag{27}$$

$$\langle (S_\alpha^z)^2 \rangle = \overline{h}^2 S(S+1) - \overline{h}\langle S_\alpha^z \rangle (1 + 2\varphi) \tag{28}$$

$$\langle (S_\alpha^z)^3 \rangle = \overline{h}^3 S(S+1)\varphi + \overline{h}^2 \langle S_\alpha^z \rangle (S(S+1) + \varphi) - \overline{h}\langle (S_\alpha^z)^2 \rangle (1 + 3\varphi). \tag{29}$$

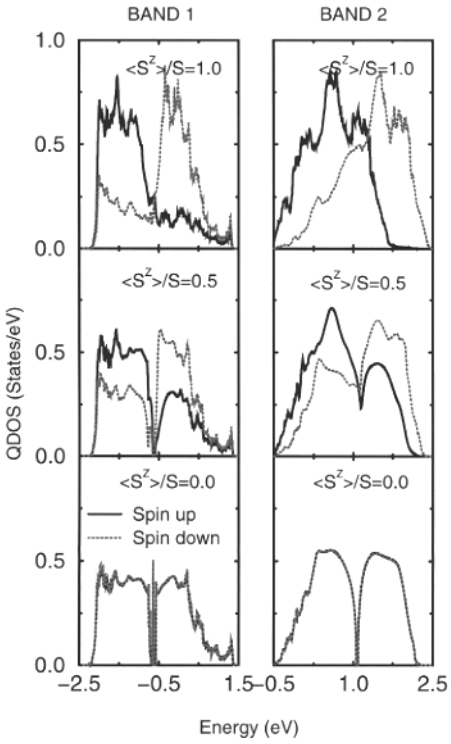

Figure 11. The sublattice quasiparticle density of states corresponding to band 1 and band 2 of EuTe for both the spins at three different f-spin magnetizations.

Some of the spin correlation functions for EuTe are plotted in figure 6. We are going to present all the other results as functions of $\langle S_\alpha^z \rangle$. For the s–f coupling constant J we have chosen a value which is commonly accepted [14, 15] as being realistic for the europium chalcogenides:

$$J = 0.2 \text{ eV}. \tag{30}$$

Let us first consider the temperature-dependent quasiparticle bandstructure, which can be read off from the spectral density peaks. Figure 7 shows the results for paramagnetic EuTe ($T = T_N$). The bandstructure is represented as a density plot to demonstrate as clearly as possible the influence of correlation effects. The degree of blackening is a measure of the height of the spectral density. Sharp and deeply black lines indicate quasiparticles of relatively long lifetimes. To demonstrate the influence of the s–f exchange interaction we have plotted for comparison in figure 8 the *uncorrelated* single-particle dispersions after decomposition into the six ('artificial') non-degenerate subbands ($m = 1, 2, \ldots, 6$). As explained above the single-particle energies have been taken from an LMTO band calculation for unpolarized, i.e., paramagnetic, EuTe. The differences from the paramagnetic quasiparticle bandstructure in figure 7 are therefore exclusively due to correlation effects conveyed by the s–f exchange interaction. The most obvious consequence of the exchange interaction is a quasiparticle damping that smears out great parts of the four dispersion branches (the four-sublattice structure produces four branches per band). As has been worked out in detail in [16] two elementary processes are responsible for finite-lifetime

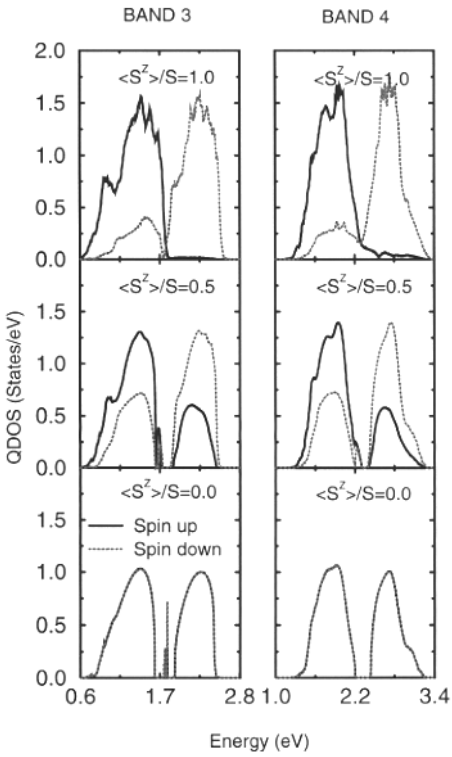

Figure 12. Same as in figure 11 but for band 3 and band 4.

effects. The majority- (minority-) spin electron can absorb (emit) a magnon thereby flipping its own spin. For the ferromagnetic counterparts this leads to a broad scattering spectrum provided there are $(-\sigma)$ states within reach which can be occupied by the original σ electron after its spinflip. The second elementary process can be described as a formation of a magnetic polaron according to a repeated emission (absorption) and reabsorption (reemission) of virtual magnons by the propagating band electron. For a ferromagnet under special circumstances ($T = 0$, $\sigma = \uparrow$) the polaron can become a stable particle, when there are no electronic $(-\sigma)$ states necessary for a decay of the polaron into a $-\sigma$ electron plus magnon. Because of the spin mixing such a situation can never arise in the antiferromagnet. In any case the polaron decays after a certain lifetime by magnon emission (absorption) without reabsorption (reemission). Besides the damping effects due to the just described spinflip processes the exchange correlation effects manifest themselves by opening a gap, which does not appear in the LMTO spectrum. Except for the $m = 6$ subband the gap appears for all subbands, and not only for the plotted symmetry directions but for the whole spectrum of the Brillouin zone as can be seen in the quasiparticle density of states. The correlation gap is temperature dependent and disappears in most cases for low temperatures (figures 9, 10).

In the case of a saturated ferromagnet ($T = 0$) the s–f problem can be solved exactly [16]. The up-spin spectrum is then very simple because the electron cannot exchange its spin with the localized and parallely aligned f system. Magnon absorption cannot happen since the saturated ferromagnet does not contain magnons. The resulting quasiparticle

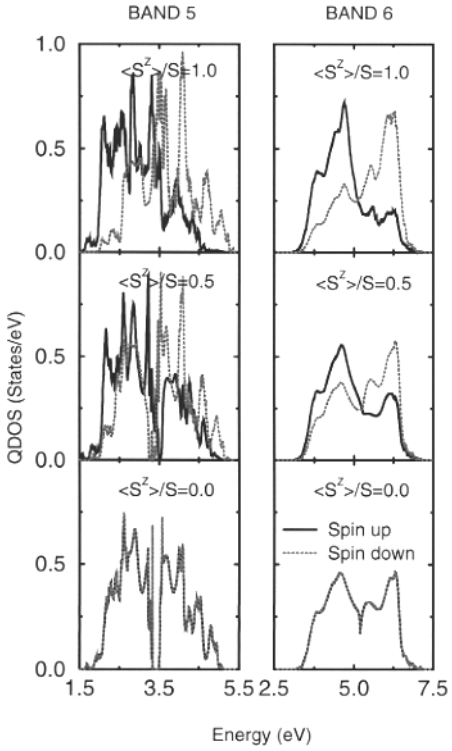

Figure 13. Same as in figure 11 but for band 5 and band 6.

bandstructure remains undeformed and only rigidly shifted with respect to the 'free' Bloch spectrum. The down-spin spectrum is more complicated because of the two above-described spinflip processes (magnon emission, polaron formation). The resulting $\downarrow$-quasiparticle bandstructure is correspondingly very much different from that of the ($\sigma = \uparrow$, $T = 0$) case. Band deformations and splittings prevent a 'Stoner-like' exchange shift of the conduction band states. The situation for the antiferromagnet comes out similarly complicated. The majority-spin electron of a certain sublattice becomes a minority-spin electron when it hops into the other sublattice. Nevertheless, for a majority-spin electron (figure 9) in a saturated sublattice the lifetime is in general higher than that of a minority-spin particle (figure 10). The majority-spin electron has the chance to move without any spinflip in its original sublattice. On the other hand, the minority-spin electron must first hop into the other sublattice to find parallel spins. The decay rate is therefore very much higher. Consequently the spectra of minority-spin electrons are drastically smeared out by quasiparticle damping. This can be recognized in the $T = 0$ quasiparticle band structure of EuTe when comparing figures 9 and 10. Contrary to the damping effects the $\uparrow$- and $\downarrow$-dispersions for a given sublattice are rather similar as concerns their positions and their shapes. Differences appear mainly in the spectral weights of the dispersions and in the just-mentioned damping. This is a characteristic of the antiferromagnet. The ferromagnet usually shows up a distinct temperature-dependent exchange splitting according to the linear term in the self-energy (22). Since the electron in the antiferromagnetic spin structure of EuTe fluctuates between majority- and minority-spin, when changing the sublattice, the up-spin and the down-spin spectra of a given sublattice bandstructure have to occupy exactly the same energy region.

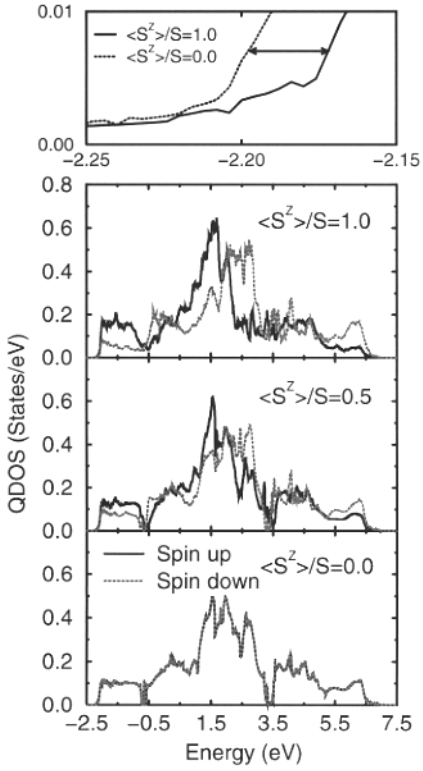

Figure 14. Total sublattice quasiparticle density of states (the sublattice density of states of all the bands added together) of EuTe for both the spins at three different f-spin magnetizations. In the upper part of the figure, the lowest part of the QDOS is shown in expanded energy scale to demonstrate the magnetic blue shift observed in EuTe.

To plot a spin resolved quasiparticle bandstructure as in figures 9, 10, e.g., means to project mixed spin states on a complete set of pure spin states. The temperature-dependent spectral weights are connected to the absolute squares of the respective expansion coefficients in the mixed spin states.

The sublattice quasiparticle densities of states are plotted in figures 11–13 for three different values of the sublattice magnetization, i.e. for three different temperatures. One recognizes that indeed for all bands and all temperatures the energy spectra coincide for both spin directions but with different densities of states. In the antiferromagnetically ordered phase ($T \leqslant T_N$) the low-energy part is dominated by the majority-spin QDOS and the high-energy part by the minority-spin QDOS. The demagnetization of the ferromagnetic sublattice with increasing temperature is due to a rearranging of the spectral weights with hardly any energy shift. The correlation caused splitting of the energy bands in the paramagnetic phase is the stronger the narrower the band. A large effective s–f coupling enhances the correlation effects. It is interesting to observe that in the case of saturated sublattice magnetization ($\langle S^z \rangle = S$) the partial bands $m = 3$ and 4 exhibit a structure very similar to that of a saturated ferromagnet (see figure 5 in [16]) indicating that the electron propagation happens mainly in the given sublattice. The high-energy part consists almost excludingly of minority spin states. The corresponding quasiparticles have hardly any chance for a spinflip

by magnon emission, representing therefore rather long-living magnetic polarons.

The total sublattice quasiparticle density of states (figure 14) is just the sum of the six subband densities of states ($m = 1, \ldots, 6$) exhibiting therewith the corresponding temperature behaviour. At two positions the correlation gaps of the ferromagnetic sublattices become visible in the total paramagnetic sublattice QDOS, too. The frequently discussed total shift of the lower conduction band edge between $T = T_N$ and $T = 0$ is very small. It turns out to be a blue shift of about -0.025 eV (see figure 14) in excellent agreement with the experiment [6].

6. Conclusions

We have derived the energy spectrum of the prototypical antiferromagnet EuTe including correlation effects and temperature dependences. Since the temperature dependences of the opposite magnetizations in different sublattices of the antiferromagnet compensate each other we have discussed our results excludingly in terms of sublattice quantities. The sublattice quasiparticle band structure has been derived from respective peaks in the spectral density. In order to get realistic spectra we have used as single-particle input of the applied interband s–f exchange model the data of a tight-binding linear muffin tin calculation. Therewith it is guaranteed that all the other interactions which are not directly accounted for by the model Hamiltonian are taken into consideration by the renormalization of the 'free' Bloch energies. For the subsequent model evaluation we used a recently proposed moment conserving Green function technique that proves to be correct in all exactly solvable limiting cases of the s–f model which are known to us.

Sublattice band structure and density of states reveal a striking temperature dependence being mainly due to the spectral weights of the energy dispersion. Minority- and majority-spin spectra exactly coincide for all temperatures but with different and strongly temperature-dependent densities of states. Between T_N and $T = 0$ the lower conduction band edge performs a small blue shift of about -0.025 eV as it is observed for EuTe in the experiment. Another temperature-dependent quantity of special interest is the quasiparticle damping that manifests itself in a broadening of the spectral density peaks. Finite lifetimes of the quasiparticles arise from spin exchange processes with the localized 4f moments either by magnon emission and absorption or by the formation of magnetic polarons.

Acknowledgment

This work has been sponsored by the 'Deutsche Forschungsgemeinschaft' under the sign AFM/EuTe.

References

[1] Wachter P 1979 *Handbook on the Physics and Chemistry of Rare Earth* vol 1, ed K A Gschneidner and L Eyring (Amsterdam: North-Holland) ch 19
[2] Haas C 1970 *CRC Crit. Rev. Solid State Sci.* **1** 47
[3] Passell L, Dietrich O W and Als-Nielsen J 1976 *Phys. Rev.* B **11** 4897
[4] Als-Nielsen J, Dietrich O W and Passell L 1976 *Phys. Rev.* B **14** 4908
[5] Dietrich O W, Als-Nielsen J and Passell L 1976 *Phys. Rev.* B **14** 4923
[6] Batlogg B, Kaldis E, Schlegel A and Wachter P 1975 *Phys. Rev.* B **12** 3940
[7] Schoenes J 1979 *J. Magn. Magn. Mater.* **11** 102
[8] Müller N, Eckstein W, Heiland W and Zinn W 1972 *Phys. Rev. Lett.* **29** 1651
[9] Kisker E, Baum G, Mahan A H, Raith W and Reihl B 1978 *Phys. Rev.* B **18** 2256

[10] Penney T, Shafer A W and Torrance J B 1972 *Phys. Rev.* B **5** 3669
[11] Schoenes J and Wachter P 1974 *Phys. Rev.* B **9** 3097
[12] Zimmer H G, Takemura K, Fischer J and Syassen K 1984 *Phys. Rev.* B **29** 2350
[13] Nolting W 1982 *Z. Phys.* B **49** 87
[14] Nolting W 1979 *Phys. Status Solidi* b **96** 11
[15] Ovchinnikov S G 1991 *Phase Transitions* **36** 15
[16] Nolting W, Mathi Jaya S and Rex S 1996 *Phys. Rev.* B **54** 14 455
[17] Nolting W, Rex S and Mathi Jaya S 1997 *J. Phys.: Condens. Matter* **9** 1301
[18] Nolting W, Borstel G and Borgiel W 1987 *Phys. Rev.* B **35** 7015
[19] Nolting W, Borgiel W and Borstel G 1987 *Phys. Rev.* B **35** 7025
[20] Nolting W, Borgiel W and Borstel G 1988 *Phys. Rev.* B **37** 7663
[21] Borstel G, Borgiel W and Nolting W 1987 *Phys. Rev.* B **36** 5301
[22] Nolting W, Dambeck T and Borstel G 1994 *Z. Phys.* B **94** 409
[23] Andersen O K 1992 *Method of Electronic Structure Calculations (ICTP Lecture Notes)*
[24] Andersen O K, Pawlowska Z and Jepsen O 1986 *Phys. Rev.* B **34** 5253
[25] Poulsen U K, Kollar J and Andersen O K 1976 *J. Phys. F: Met. Phys.* **6** L241
[26] Janak J F and Williams A R 1976 *Phys. Rev.* B **14** 4199
[27] Bei der Kellen S, Nolting W and Borstel G 1990 *Phys. Rev.* B **42** 447
[28] Kim B, Andrews A B, Erskine J L, Kim K J and Harmon B N 1992 *Phys. Rev. Lett.* **68** 1931
[29] Callen H B 1963 *Phys. Rev.* **130** 890